A Flow Graph Analysis of 3-and 4-Port Junction Circulators

SVEN HAGELIN, MEMBER, IEEE

Abstract—A simple theoretical model of a lossless nonideal junction circulator is described. The model consists of a matched lossless n-port junction with a lossless two-port connected to each arm. The basic thought behind it is to separate the reflecting properties of the circulator from the other ones. For the case $n=3$, unsymmetrical as well as symmetrical junctions are treated. For a symmetrical three-port, the justification of the model has also been experimentally verified. In the case $n=4$, a symmetrical junction is treated. Flow graphs are used for visualizing the scattering matrices of combined networks and for calculating the coefficients of them.

I. Introduction

Several authors have considered the network properties of circulators and some interesting results have been obtained, most of them expressed in terms of scattering parameters. The possibility of synthesizing an ideal circulator from a general lossless n-port junction of transmission lines has attracted the highest interest [1]–[4]. However, the practical circulator is different from the ideal one. It is true that in some cases it may have such good characteristics that its deviation from ideal performance may be neglected. But often only a small change in temperature, signal power level, or signal frequency is enough to make the approximation inapplicable. Thus, it is necessary to give attention also to nonideal circulators.

In this paper we shall consider a simple theoretical model of a lossless n-port junction (not necessarily symmetrical) which exhibits nonideal circulation. The model consists of a matched lossless n-port junction with a lossless two-port connected to each arm. The case $n=3$ is the most common in practice, and for this case we shall discuss first unsymmetrical and then symmetrical junctions. For a symmetrical three-port, the justification of the model has also been experimentally verified. In the case $n=4$, the analysis is restricted to symmetrical junctions for the sake of simplicity. The model is applicable also for networks with more than four ports, but the mathematical treatment becomes rather involved. However, the model may still be useful for qualitative understanding of general circulator properties.

Manuscript received August 30, 1965; revised February 17, 1966. The work reported was carried out at the Research Institute of National Defence (FOA), Sweden.
The author is with the Research Institute of National Defence (FOA), Stockholm, Sweden.

II. Properties of a Symmetrical Lossless Three-Port

As a background to the description of the three-port circulator model, we shall consider the properties of a lossless three-port network and see what information can be found on nonideal circulators. To reduce the number of parameters, we limit ourselves to symmetrical three-ports.

For a lossless symmetrical three-port, the following well-known relations are valid:

$$A^2 + B^2 + C^2 = 1 \tag{1}$$

$$ab^* + bc^* + ca^* = 0 \tag{2}$$

where $a=A\cdot e^{j\alpha}$, $b=B\cdot e^{j\beta}$, and $c=C\cdot e^{j\gamma}$ are the scattering coefficients. When the reflection coefficient $a=0$, (1) and (2) give $B=1$ and $C=0$ (or vice versa), which means ideal circulation.

In order to find out something about nonideal circulators, we solve (1) and (2). If the value of B from (1) is inserted in (2), we obtain, after some rearrangements,

$$(A^2 + C^2 + \kappa AC)^2 - [A^2 + C^2 + 2\kappa AC - A^2C^2(1-\kappa^2)] = 0 \tag{3}$$

where $\kappa = \cos(2\beta-\alpha-\gamma)$. For a fixed value of κ, (3) represents a line in the (A, C)-plane. In Fig. 1 this line is shown for some values of κ. As κ can only vary from -1 to $+1$, all possible lines define a closed region, where all realizable lossless symmetrical three-ports can be found. When $\kappa=\pm 1$, (3) becomes

$$A^2 + C^2 + AC \pm (A + C) = 0$$
$$A^2 + C^2 - AC \pm (A - C) = 0. \tag{4}$$

These equations, representing the boundary lines of the allowed region, were first derived by Butterweck [5].

The working point of an ideal circulator ($A=C=0$) is situated at the origin of Fig. 1, while it is situated near the origin in the allowed region for a nonideal circulator. The ratio of C to A is of special interest in this area. For that reason $C/A=f(A)$ for $\kappa=-1$, $\kappa=-0.99$, and $\kappa=-0.97$ has been calculated from (3) and can be seen in Fig. 2. Further, for some other values of κ the points where $C/A=1$ have been indicated.

We observe that the maximum error in the often used relation $A\approx C$ [6] is considerable even when the mis-

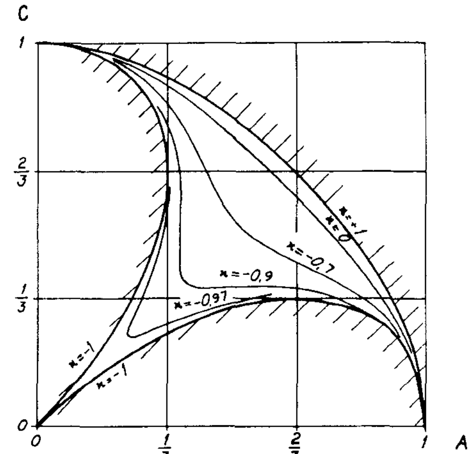

Fig. 1. The closed region of realizable lossless symmetrical three-ports in the (A, C)-plane.

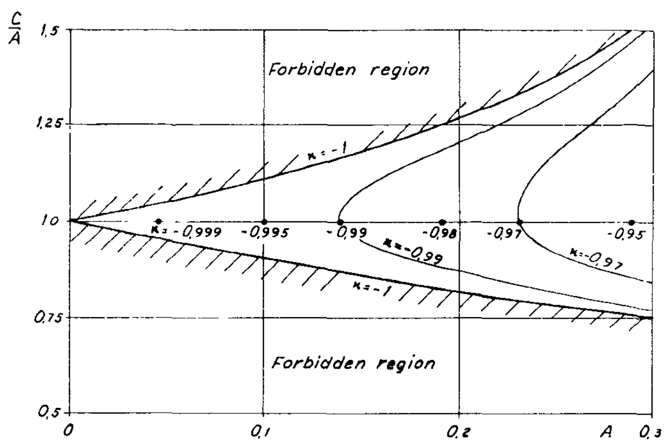

Fig. 2. The ratio C/A as a function of A for $\kappa=-1$, $\kappa=-0.99$, and $\kappa=-0.97$.

match is rather small. Equation (3) gives an exact relation between A and C but, as the value of κ is not easily obtained, it is of little value in practice.

III. Theoretical Model of a Three-Port Circulator

We shall now proceed to describe a simple theoretical model of a nonideal three-port circulator consisting of a lossless three-port with a lossless two-port connected to each arm. The basic thought behind the model is to separate the reflecting properties of the circulator from the other ones. The function of the two-ports is accordingly to determine the degree of matching, while the interior network is assumed to be intrinsically matched, i.e., it is an ideal circulator. How good a circulator the whole device is depends, consequently, on the properties of the two-ports.

For the three-port, the scattering coefficients in the three transmission directions are denoted by $b_i=e^{j\beta_i}$ $(i=1, 2, 3)$. For lossless two-ports with special reference planes, the scattering matrix can be written with only two real parameters [7]:

$$(S) = \begin{pmatrix} r_i & n_i \\ m_i & t_i \end{pmatrix} = \begin{pmatrix} R_i & \sqrt{1-R_i^2}\cdot e^{j\phi_i} \\ -\sqrt{1-R_i^2}\cdot e^{-j\phi_i} & R_i \end{pmatrix} \tag{5}$$

where $(i=1, 2, 3)$. R_i is the modulus of r_i and t_i. ϕ_i is a phase angle that may be considered arbitrary for the needs of this paper.

The use of flow graphs for visualizing scattering matrices is very advantageous, especially when the problem is to determine the scattering matrix of a combination of networks with known scattering matrices. The coefficients in the total scattering matrix may then be calculated using Mason's "nontouching loop rule" [8]. In Fig. 3 the flow graph of the three-port circulator model is shown. The reference planes of the three-port are chosen to coincide with the reference planes of the corresponding two-ports. E^i and E^r stand for incident and reflected signals in each arm. The following expressions for the scattering coefficients of the whole network can now be obtained:

$$S_{11} = r_1 + \frac{m_1 n_1 b_1 b_2 b_3 t_2 t_3}{N} \tag{6}$$

$$S_{21} = \frac{m_1 n_2 b_1}{N} \tag{7}$$

$$S_{31} = \frac{m_1 n_3 b_1 b_2 t_2}{N} \tag{8}$$

$$S_{12} = \frac{m_2 n_1 b_2 b_3 t_3}{N} \tag{9}$$

$$S_{22} = r_2 + \frac{m_2 n_2 b_1 b_2 b_3 t_1 t_3}{N} \tag{10}$$

$$S_{32} = \frac{m_2 n_3 b_2}{N} \tag{11}$$

$$S_{13} = \frac{m_3 n_1 b_3}{N} \tag{12}$$

$$S_{23} = \frac{m_3 n_2 b_1 b_3 t_1}{N} \tag{13}$$

$$S_{33} = r_3 + \frac{m_3 n_3 b_1 b_2 b_3 t_1 t_2}{N} \tag{14}$$

where $N=1-b_1b_2b_3t_1t_2t_3$. If the values of r_i, m_i, n_i, and t_i from (5) are inserted together with $b_i=e^{j\beta_i}$, the absolute values of (6)–(14) are expressed as functions of the parameters R_1, R_2, R_3, and ϑ, where $\vartheta=(\beta_1+\beta_2+\beta_3)/3$. These parameters may be measured in an easy way. If (13) is divided by (11), the result is

$$\frac{S_{23}}{S_{32}} = \frac{m_3 n_2 b_1 b_3 t_1}{m_2 n_3 b_2} = R_1 \cdot e^{j(\beta_1+\beta_3-\beta_2+2\phi_2-2\phi_3)}. \tag{15}$$

Consequently, the value of R_1 is obtainable by mea-

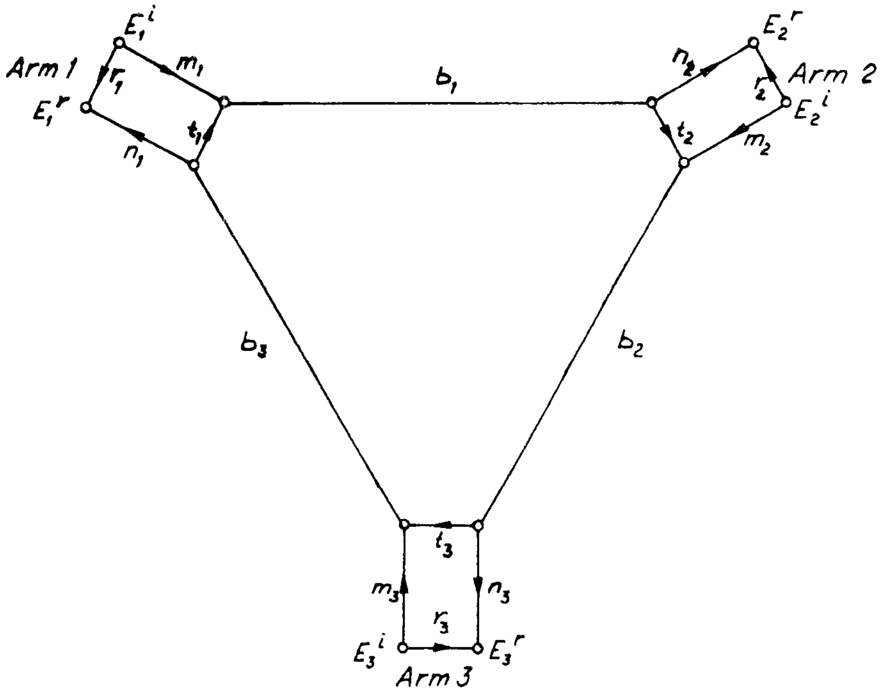

Fig. 3. Flow graph for a lossless three-port with a two-port connected to each arm.

suring the ratio of S_{23} to S_{32}. In the same way, R_2 and R_3 can be found from S_{31}/S_{13} and S_{12}/S_{21}. If the phase angles of these three ratios are also measured, the value of ϑ can be calculated, because

$$\frac{S_{23}}{S_{32}}\cdot\frac{S_{31}}{S_{13}}\cdot\frac{S_{12}}{S_{21}} = R_1\cdot R_2\cdot R_3\cdot e^{j(\beta_1+\beta_2+\beta_3)} = R_1\cdot R_2\cdot R_3\cdot e^{j3\vartheta}. \quad (16)$$

In the symmetrical case, where the three two-ports are equal and the three-port is symmetrical, all subscripts in the right-hand members of (6)–(14) may be discarded, and the nine scattering coefficients are reduced to three, which we call S_1, S_2, and S_3. Instead of (15) and (16) we obtain

$$\frac{S_3}{S_2} = b\cdot t = R\cdot e^{j\vartheta}. \quad (17)$$

Here only two parameters, R and ϑ, are enough for determination of the scattering coefficients.

As we studied the ratio C/A for nonideal symmetrical circulators in Section II, we shall do the same thing with $|S_3|/|S_1|$ for the model. The modulus of the ratio of (8) to (6) is in the symmetrical case

$$\frac{|S_3|}{|S_1|} = \frac{1 - R^2}{\sqrt{1 + R^2 - 2R\cos 3\vartheta}}\cdot \quad (18)$$

In Fig. 4, (18) is pictured graphically. When the circulator is ideal ($R=0$), $|S_3|/|S_1|$ becomes equal to 1 as did C/A in Fig. 2. When $R\neq 0$, ϑ has an essential influence on $|S_3|/|S_1|$. The boundary lines of the allowed region are obtained for $\cos 3\vartheta = \pm 1$ and they are $|S_3|/|S_1| = 1 \pm R$.

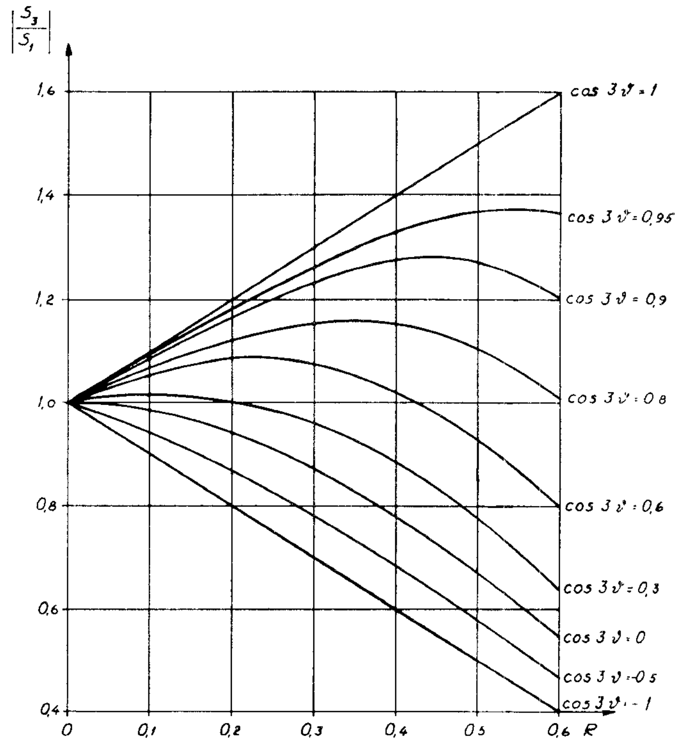

Fig. 4. Equation (18) in graphical representation.

IV. Experimental Results Compared with the Three-Port Circulator Model

The practical value of a theoretical model depends first of all on the extent of its relation to reality. To evaluate this, R and ϑ have been determined by measuring the ratio of S_3 to S_2 on a simple symmetrical circulator configuration. If R and ϑ for a particular frequency are known, a theoretical value of $|S_1|$ can be found from (6) and can be compared to a measured one. However, in order to obtain a more clear graphical picture, the comparison has been made between (18) and measured values of $|S_3|/|S_1|$.

The chosen circulator configuration consists of two transversely magnetized circular ferrite disks which are symmetrically located at the center of the upper and lower waveguide wall in an X-band waveguide Y-junction. In this case, the theoretical model may be physically interpreted as can be seen in Fig. 5, where the flow graph has been projected on a ferrite disk. The matched three-port corresponds to the interior of the disk. The edge of the disk constitutes a discontinuity for the signal in each arm and is represented by the two-ports. Inside the ferrite only phase shift will affect the signal.

Accurate measurements of the data of the circulator configuration have been made over the frequency range 8.3—11.0 GHz. The results are shown in Fig. 6. As usual, when no special matching procedures have been made, circulation only occurs over a narrow frequency band centered around 9.04 GHz. For this frequency the data are: isolation 46.3 dB, insertion loss 0.10 dB, and VSWR = 1.025. On both sides of the center frequency the circulation gradually deteriorates. At about 10.3 GHz, the device is reciprocal; for further increase of frequency, circulation appears in the other direction.

Although the model is made for a lossless junction, it is valid even when small losses are present. The only difference from the ideal case is that $|b| \neq 1$. As can be seen from (17), this has only a small influence on R as long as $|b|$ has a value close to 1. If precise values of R are required, one can correct the measured value of S_3/S_2 by the losses. In this case, the losses are so small —0.10–0.15 dB or 2–3 percent of the incident signal power—that a correction is not necessary.

From the data in Fig. 6, values of R have been calculated and are shown in Fig. 7. Values of ϑ have been determined from measurements of the phase difference between the two transmission directions (Fig. 8). A step of about 180° occurs at the circulation frequency, which means a change of sign for cos 3ϑ.

Now when R and ϑ are known, $|S_3|/|S_1|$ for every measuring frequency can be calculated from (18). For the same frequencies experimental values for comparison with the theoretical ones have been obtained from the data in Fig. 6. The two sets of values are shown in Fig. 9 as a function of $|S_1|$. At low frequencies $|S_3|/|S_1| < 1$, while at high frequencies $|S_3|/|S_1| > 1$. In the model this is due to the change of sign of cos 3ϑ. At the circulation frequency $|S_3|/|S_1| \approx 1$, which agrees with Fig. 2 and Fig. 4. The close fit between measured and calculated values confirms that the interior phase shift ϑ has a considerable influence on $|S_3|/|S_1|$. This can be said to prove that the circulator model is justified and applicable in theoretical study of nonideal circulators. It gives a simple relation between the reflection coefficient and the isolation for a three-port with nonideal circulation. The relation uses parameters that can be easily measured.

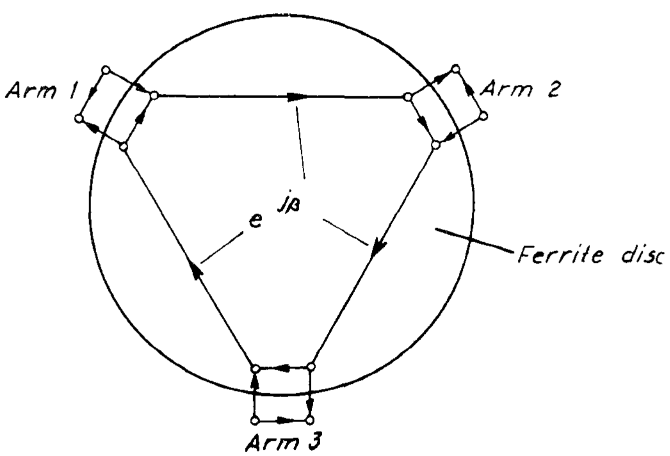

Fig. 5. Model of a circulator ferrite disk, where the ferrite edge is represented by a general two-port and the interior of the ferrite by a matched three-port.

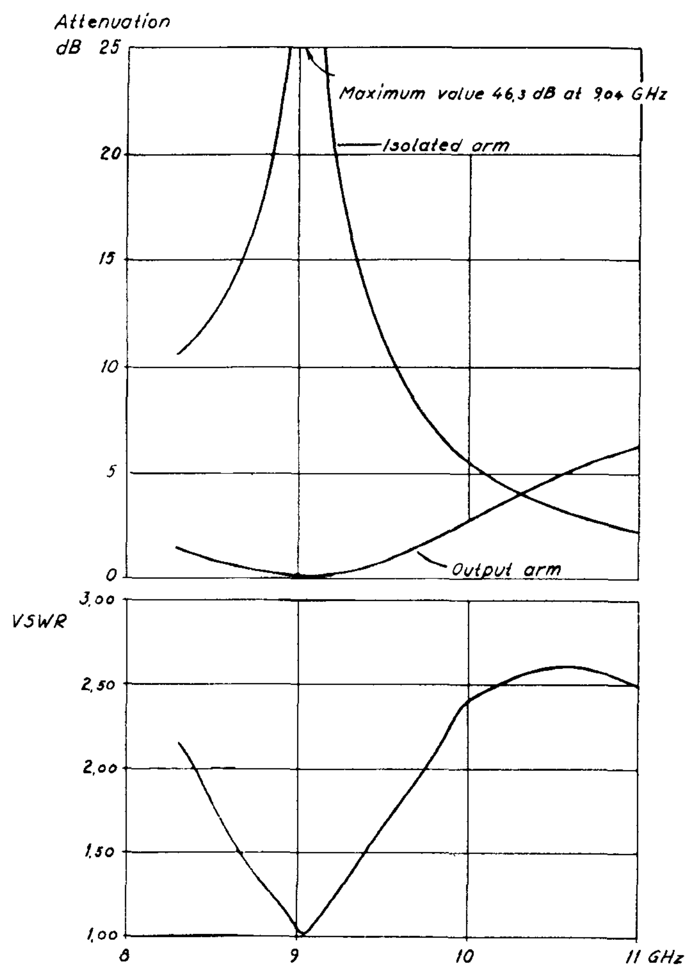

Fig. 6. Variation of attenuation and VSWR with frequency for circulator configuration.

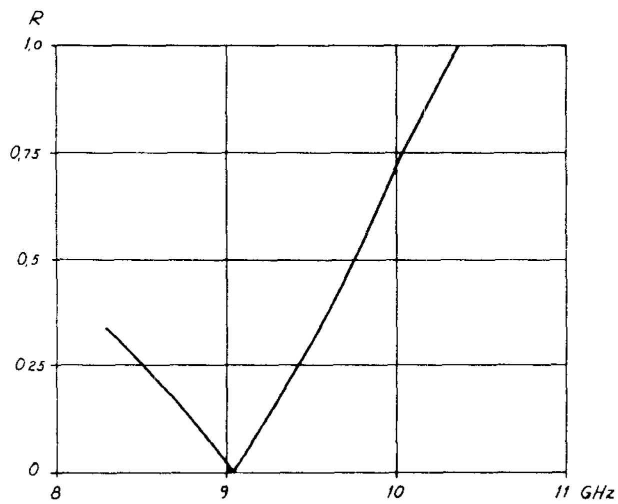

Fig. 7. R as a function of frequency.

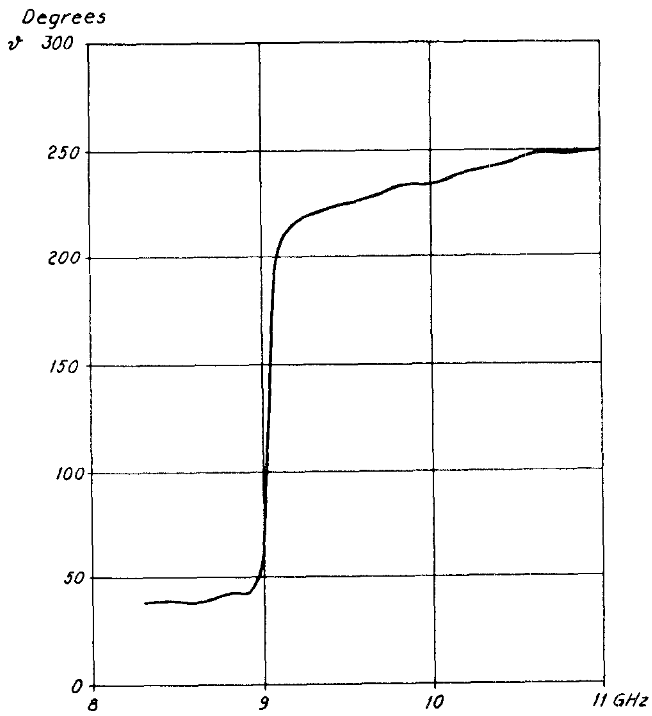

Fig. 8. Differential phase shift ϑ between S_3 and S_2 for a waveguide circulator.

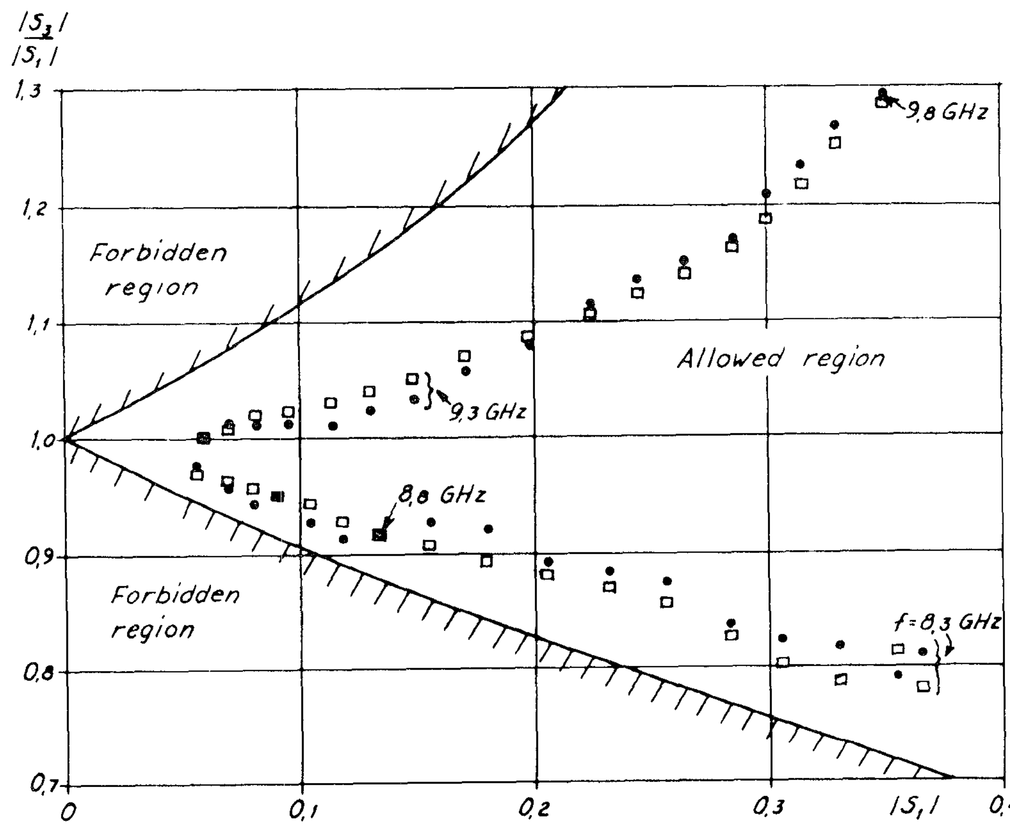

Fig. 9. Comparison between calculated values (squares) and measured values (dots) of $|S_3|/|S_1|$.

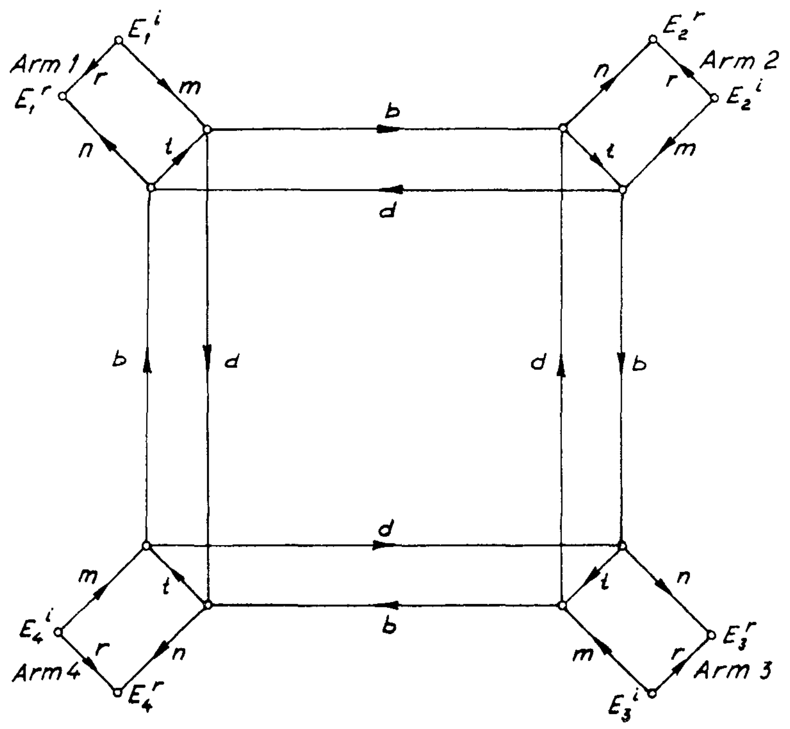

Fig. 10. Flow graph for a matched nonreciprocal symmetrical four-port with a two-port connected to each arm.

V. Theoretical Model of a Four-Port Circulator

A model of a four-port circulator can be based on the same reasoning as in the case of three-port. We begin by stating that the scattering matrix of a symmetrical four-port may be written:

$$(S) = \begin{bmatrix} a & d & c & b \\ b & a & d & c \\ c & b & a & d \\ d & c & b & a \end{bmatrix} \qquad (19)$$

where the new parameter $d = D \cdot e^{i\delta}$. If the four-port is matched and the losses are zero, the following relations between the coefficients of (S) are valid:

$$B^2 + C^2 + D^2 = 1 \qquad (20)$$

$$bc^* + cd^* = 0 \qquad (21)$$

$$bd^* + db^* = 0. \qquad (22)$$

Equation (21) demands that $C = 0$ or $B = D$. The latter cannot be true for a nonreciprocal four-port, and thus we put $C = 0$. Equations (20) and (22) then give

$$\left.\begin{aligned} B &= \sqrt{1 - D^2} \\ 2\beta &= 2\delta \pm \pi \end{aligned}\right\} . \qquad (23)$$

To the arms of this matched four-port are connected four equal lossless two-ports. The resulting flow graph is shown in Fig. 10. The scattering matrix for the whole device has the same principal appearance as (19), but the coefficients are in this case denoted by S_1, S_2, S_3, and S_4. They are found to be

$$S_1 = r + mn \cdot \frac{2bdt + (b^2 - d^2)^2 t^3}{N} \qquad (24)$$

$$S_2 = mn \cdot \frac{b - dt^2(b^2 - d^2)}{N} \qquad (25)$$

$$S_3 = mn \cdot \frac{t \cdot (b^2 + d^2)}{N} \qquad (26)$$

$$S_4 = mn \cdot \frac{d + bt^2(b^2 - d^2)}{N} \qquad (27)$$

where $N = 1 - 4bdt^2 - (b^2 - d^2)^2 \cdot t^4$.

To study the ratios of $|S_2|$, $|S_3|$, and $|S_4|$, we insert the values of r, m, n, t, and b from (5) and (23). The results are

$$\frac{|S_3|}{|S_2|} = \frac{R(1 - 2D^2)}{\sqrt{1 - D^2 + D^2R^4 + 2 \cdot \sqrt{1 - D^2} \cdot DR^2 \cdot \cos\eta}} \qquad (28)$$

$$\frac{|S_4|}{|S_2|} = \sqrt{\frac{D^2 + R^4(1 - D^2) + 2 \cdot \sqrt{1 - D^2} \cdot DR^2 \cdot \cos\eta}{1 - D^2 + D^2R^4 + 2\sqrt{1 - D^2} \cdot DR^2 \cos\eta}} \qquad (29)$$

where $\eta = 3\delta - \beta$ and $0 \leq D^2 < 0.5$ (for the circulation direction $1 \to 2 \to 3 \to 4 \to 1$). Thus, three parameters are necessary to describe the properties of the four-port circulator. The parameter D controls the distribution of the power in the internal four-port. If $D = 0$, then $|S_3|/|S_2| = R$ and $|S_4|/|S_2| = R^2$. On the other hand, if $R = 0$, then

$$\frac{|S_3|}{|S_2|} = 0 \quad \text{and} \quad \frac{|S_4|}{|S_2|} = \frac{D}{\sqrt{1 - D^2}} .$$

Hence, only one of the output arms may be isolated by matching. The parameter η represents the phase shift in the internal four-port and can have essential influence on the possibilities to minimize $|S_4|$ when both D and R differ from zero.

The validity of the four-port circulator model has not been experimentally verified, but there is no reason to believe that there is a difference between the three- and four-port models in this respect.

VI. Conclusion

The method of transforming a nonreciprocal lossless three-port into an ideal circulator by connecting appropriate external two-ports to each arm is easily understandable if the three-port in question is represented by its model. In that case, the network consists of an ideal circulator with two cascaded two-ports connected to each arm. It is clear that if the outer two-port has the appropriate characteristics, it will cancel the reflections from the inner two-port and the whole device will appear to be matched. It is also easy to see why this method is not sufficient for junctions with more than three arms. If external two-ports are connected to each arm in the flow graph in Fig. 10 so that the reflections disappear, the network will not represent a circulator. Only one of the output arms can be isolated in this way.

It has been shown in Section II that the phase shift has a considerable influence on the properties of a general lossless three-port network. Also, in the models of the three- and four-port circulators, the phase shift has great influence and it appears in a form that can be easily measured. It is then possible to describe the relation between isolation and reflection coefficient of a nonideal three-port circulator more exactly than if the relation $A \approx C$ is used.

VII. Acknowledgment

The author wishes to thank P. E. Ljung for many valuable suggestions and ideas and for reading the manuscript, and D. Thunqvist for many interesting discussions.

References

[1] B. A. Auld, "The synthesis of symmetrical waveguide circulators," *IRE Transactions on Microwave Theory and Techniques*, vol. MTT-7, pp. 238–246, April 1959.
[2] U. Milano, J. H. Saunders, and L. Davis, "A *Y*-junction stripline circulator," *IRE Transactions on Microwave Theory and Techniques*, vol. MTT-8, pp. 346–350, May 1960.
[3] P. Penfield, Jr., "A classification of lossless three-ports," *IRE Transactions on Circuit Theory*, vol. CT-9, pp. 215–223, September 1962.
[4] B. L. Humphreys and J. B. Davies, "The synthesis of *N*-port circulators," *IRE Transactions on Microwave Theory and Techniques*, vol. MTT-10, pp. 551–554, November 1962.
[5] H. J. Butterweck, "Der *Y*-Zirkulator," *Arch. Elekt. Ubertragung (Germany)*, vol. 17, pp. 163–176, April, 1963.
[6] J. B. Thaxter and G. S. Heller, "Circulators at 70 and 140 KMC," *Proc. IRE (Correspondence)*, vol. 48, pp. 110–111, January 1960.
[7] B. Lax and K. Button, *Microwave Ferrites and Ferrimagnetics*. New York: McGraw-Hill, 1962, Sec. 11-4.
[8] S. J. Mason, "Feedback theory—Further properties of signal flow graphs," *Proc. IRE*, vol. 44, pp. 920–926, July 1956.

Correction

J. Paul Shelton, Jr., author of the paper "Impedances of Offset Parallel-Coupled Strip Transmission Lines," which appeared in these Transactions, vol. MTT-14, no. 1, January 1966, pp. 7–14, is indebted to Steven March for his careful reading of the paper and pointing out the following.

References [4] and [6] should be interchanged.

Under *Derivation for Loose Coupling*, bottom of the first column, page 10, the equation from ΔC should read:

$$\Delta C = C_0 - C_e = \frac{120\pi}{\sqrt{\epsilon_r} Z_0}\left(\frac{\rho - 1}{\sqrt{\rho}}\right) \qquad \text{[from (7)]}$$

$$= \frac{2}{\pi} \log\left(\frac{1 + aq}{aq}\right). \qquad \text{[from (3), (4), and (9)]}$$

The last paragraph under *Derivation for Loose Coupling* should read:

The explicit solution for loose coupling, given Z_0, ϵ_r, ρ, and s, is now accomplished by solving (9) for ΔC, (15) for k, (16) and a and q, (3) or (4) for C_{f0} and C_{fe}, (9) for w, and (6) for w_c.